Nano-Structures & Nano-Objects 1 (2015) 24–31

Contents lists available at ScienceDirect

Nano-Structures & Nano-Objects

journal homepage: www.elsevier.com/locate/nanoso

Bis((dialkylamino)alkylselenolato)metal complexes as precursors for microwave-assisted synthesis of semiconductor metal selenide nanoparticles of zinc and cadmium in the ionic liquid [BMIm][BF_4]

Karsten Klauke [a], Björn Hahn [a], Kai Schütte [a], Juri Barthel [b], Christoph Janiak [a,*]

[a] Institut für Anorganische Chemie und Strukturchemie, Heinrich-Heine Universität Düsseldorf, Universitätsstraße 1, D-40225 Düsseldorf, Germany

[b] Gemeinschaftslabor für Elektronenmikroskopie RWTH-Aachen, Ernst-Ruska-Centrum für Mikroskopie und Spektroskopie mit Elektronen, D-52425, Jülich, Germany

HIGHLIGHTS

- (Dialkylamino)alkylselenolates as new single-source precursors for ZnSe and CdSe-NPs.
- ZnSe- and CdSe-NPs were obtained by microwave irradiation of precursor/IL suspensions.
- Obtained particles were mostly spherical, crystalline and only slightly agglomerated.
- No further stabilizing agents needed and no formation of metal fluorides observed.
- For ZnSe the particle diameter was 4–7 nm, while for CdSe the diameter was 10–19 nm.

GRAPHICAL ABSTRACT

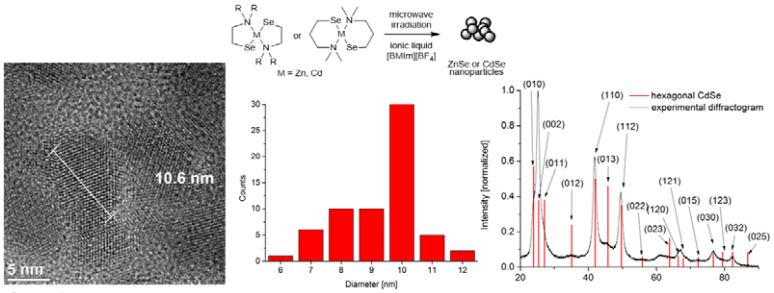

Synopsis:
Bis(dialkylamino)alkylselenolates are novel single-source precursors for ZnSe and CdSe-nanoparticles by microwave irradiation of precursor/IL dispersions.

ARTICLE INFO

Article history:
Received 3 February 2015
Received in revised form
6 May 2015
Accepted 7 June 2015

Dedicated to Prof. Dr. Manfred Scheer on the occassion of his 60th birthday

Keywords:
Metal selenide
Ionic liquid
Zinc selenide
Cadmium selenide
Microwave irradiation
Nanoparticles

ABSTRACT

Based on (dimethylamino)ethyldiselenide, (diethylamino)ethyldiselenide and (dimethylamino)propyldiselenide six different bis(dialkylamino)alkylselenolates with zinc and cadmium were decomposed by microwave irradiation in the ionic liquid (IL) 1-butyl-3-methyl-imidazolium tetrafluoridoborate ([BMIm][BF_4]) to give the respective metal selenide nanoparticles. In comparison to common methods like the hot injection method attention was paid how variations of the ligand system and different decomposition times affect the nanoparticle synthesis with respect to size, shape, crystallinity and crystal phase. The decomposition of the single-source zinc and cadmium precursors in the fluorous IL led mostly to spherical, crystalline and only slightly agglomerated nanoparticles. No formation of ZnF_2 or CdF_2 was observed which is different from the known dual-source synthesis. In case of the zinc precursors, hexagonal and cubic ZnSe with a particle diameter between 4–7 nm were obtained, whereas in case of the cadmium precursors hexagonal CdSe with an average particle diameter of 10–19 nm were prepared. An increase in decomposition time from 5 to 15 min at 250 °C mostly led to similar results concerning the particle size and crystal phase which is different from the hot injection method, thereby suggesting that the IL has a decisive role for nanocrystal growth and stabilization. No further stabilizing agents were necessary to reproducibly prepare ZnSe or CdSe particles with an average diameter below 10 or 20 nm,

* Corresponding author. Fax: +49 0 211 8112287.
E-mail address: janiak@uni-duesseldorf.de (C. Janiak).

http://dx.doi.org/10.1016/j.nanoso.2015.06.001
2352-507X/© 2015 Elsevier B.V. This is an open access article under the CC BY-NC-ND license (http://creativecommons.org/licenses/by-nc-nd/4.0/).

respectively. All dispersions of the metal selenide nanoparticles in [BMIm][BF_4] were characterized by high resolution transmission electron microscopy (HR-TEM), energy dispersive X-ray spectroscopy (EDX) and X-ray powder diffraction (PXRD).

© 2015 Elsevier B.V.
This is an open access article under the CC BY-NC-ND license (http://creativecommons.org/licenses/by-nc-nd/4.0/).

1. Introduction

One of the emerging areas of nanotechnology is the field of semiconductor nanoparticles, whose interesting properties have attracted much attention in the past few decades. One of the most important concepts in relation to semiconductor nanoparticles is the quantum confinement which describes the particle-size-depended discretization of the electronic energy levels. Among others this has direct influence on the thermoelectric and optoelectric properties the material. Therefore, due to various possible applications especially II–VI and IV–VI semiconductors such as ZnSe, CdSe or PbSe belong to the best studied systems of this class of materials. They can be used in LEDs, photovoltaics, biological imaging, thermoelectric devices or single-electron transistors [1–11]. In terms of selenium-containing semiconductor nanoparticles a wide variety of starting materials is known [1,12–14]. In the literature metal selenide nanoparticles are mostly prepared by a dual-source approach from the reaction of different metal salts like MSO_4 or $M(OAc)_2$ and Na_2SeO_3 [1,15]. The metal complexes of aminoalkylselenoles like selenocysteamine for example have proven to be excellent single-source precursors for the preparation of metal selenide nanoparticles. Most of these complexes are air and moisture stable solids with moderate decomposition temperatures and are easily synthesized through cleavage of the respective diselenide (Scheme 1) [12–14].

One of the main goals of nanomaterial science is to develop economically and environmentally efficient methods for the design of novel nanostructured materials, preparation of thin films and highly dispersed systems, as well as the fabrication of functional nanostructures. Common methods for the synthesis of semiconductor nanoparticles include ball milling and chemical vapor deposition processes as well as precipitation methods. In wet chemical precipitation, sterically demanding stabilizing agents like hexadecylamine (HDA) or trioctylphosphine oxide (TOPO) have to be used to stabilize the nanoparticles and to prevent agglomeration. Another notable fact is, that in other methods like the classical hot injection method the particle size increases drastically with the reaction time, except when working in non-coordinating solvents like 1-octadecene, where the final size is quickly reached and remains stable for long time [1].

Due to their unique physicochemical properties ionic liquids, especially room temperature ionic liquids like 1-butyl-3-methylimidazolium tetrafluoridoborate, [BMIm][BF_4], have recently received attention as media for the synthesis of different types of nanoparticles [16–21] and inorganic materials [22,23] such as metal oxides including ZnO [24] or CuO semiconductor nanoparticles [25,26], metal chalcogenides [27,28], polynuclear metal complexes [29–31]. Among others, the properties of ILs include a high dielectric constant, polarity, thermal stability and a negligible vapor pressure. The stabilization of nanoparticles in ionic liquids is based on the integration of the particles in the network-like structure of the ionic liquid by weakly coordinating interactions, resulting in an enhancement of the repulsive energy [32–34]. Furthermore, through choice of the anion and cation, ionic liquids can be specifically designed for different tasks. Accordingly, a variety of different techniques and methods has been employed, including solvothermal [35–38], sol–gel [39–41], electrodeposition [42,43] and radiation assisted syntheses [44–50]. However, reports about the preparation of semiconductor nanoparticles in ionic liquids are quite rare [15,27,51,52]. There are gaps, for example in the selection of suitable precursors and methods, as well as in the investigation of the growth and shape-determining processes. Although ionic liquids are still expensive, their recycling makes progress and ILs are often considered a "green" alternative to classical organic solvents due to their less-harmful nature [53]. Therefore, we describe here for the first time the microwave assisted decomposition of single-source (alkylamino)alkylselenolates precursors of zinc and cadmium (**1**–**6**) in an ionic liquid, here [BMIm][BF_4]. Initial attempts to form MSe from metal acetate hydrates and bis(dialkylamino)alkyldiselenides in a dual-source approach yielded samples where the X-ray powder diffraction pattern showed the formation of MSe (M = Zn or Cd), albeit together with MF_2 impurities from the reaction with the BF_4^- anion of the IL (Figure S1 in Suppl. Mater.). In the literature the formation of MF_2 impurities is prevented through the use of non-fluoride containing ILs, such as [BMIm][$EtSO_4$] [15].

In this work we test the single-source approach to prevent the formation of metal fluorides from BF_4^- in the fluorous IL. Different from most other methods like the hot injection method we show that variations in ligand system of the precursor and different decomposition times do not affect the nanoparticle synthesis in the IL. Also, no further stabilizing agents are needed to reproducibly prepare MSe particles with average diameters of less than 20 nm.

2. Results and discussion

2.1. Precursor compounds

The synthesis of the bis((dialkylamino)alkylselenolato)metal(II) compounds is depicted in Scheme 1 and follows the literature [12,13,54].

2.2. Thermogravimetric analysis of Zn complexes **1–3**

The thermogravimetric analysis of the prepared bis((dialkylamino)alkylselenolato)zinc(II) complexes (**1**–**3**) (Fig. 1) verifies their decomposition temperature of about 250 °C, which corresponds to similar zinc selenolate complexes in the literature [13]. The residual mass (Δm) is close to the expected values for ZnSe ($\Delta m_{\text{theor.}}$), as shown in Table 1. Also formation of ZnSe as decomposition product was positively identified by X-ray powder diffraction of the residues (Figure S2 in Suppl. Mater.). The diffraction patterns showed the formation of either hexagonal or cubic ZnSe (Table 1).

2.3. ZnSe-NPs in [BMIm][BF_4]

Dispersions of pure ZnSe nanoparticles in [BMIm][BF_4] were obtained by suspending a defined amount of the respective precursor in the ionic liquid and then decomposing it via microwave assisted heating for 5 or 15 min at 250 °C as shown in Scheme 2.

Table 1
Thermogravimetric analyses of selenolate zinc precursors **(1–3)** and crystal phase of ZnSe formed.

Precursor	Δm [%]	$\Delta m_{theor.}$ [%]	Decomp. temp. (° C)	ZnSe crystal system[a]
1	43	39	220	hexagonal $P6_3mc$
2	48	45	210	cubic F-43m
3	43	43	215	cubic F-43m

[a] From PXRD analysis of the residue of the thermal analysis (cubic ZnSe, reference: COD-database: 9008857; hexagonal ZnSe, reference: COD-database: 9008879).

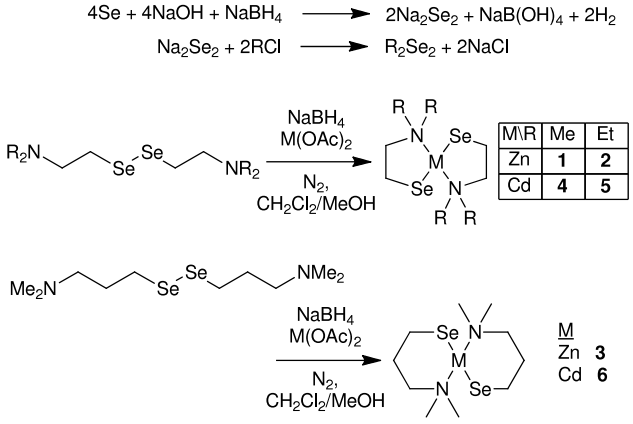

Scheme 1. Synthesis of the bis((dialkylamino)alkylselenolato)metal(II) precursors.

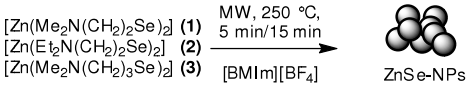

Scheme 2. Decomposition of the bis((dialkylamino)alkylselenolato)zinc(II) complexes (**1**–**3**) to ZnSe-NPs.

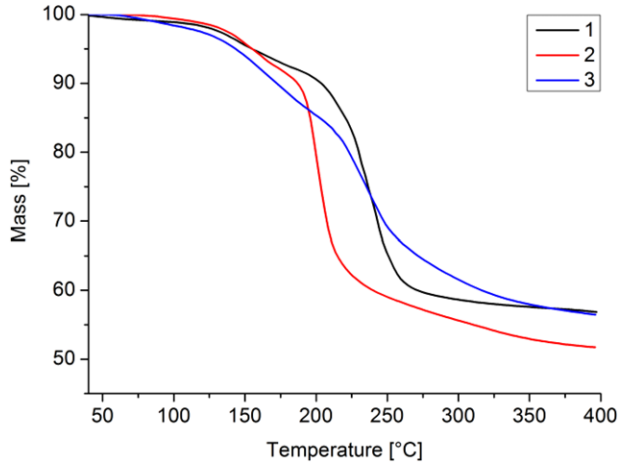

Fig. 1. Thermogravimetric analyses of bis((alkylamino)alkylselenolato)zinc(II) complexes (**1**–**3**).

In Fig. 2 the HR-TEM images of ZnSe nanoparticles obtained after the decomposition of **2** for 5 min indicate agglomerated, spherical and crystalline particles with a diameter distribution of 4.7 ± 1.3 nm. The particle diameter determined by the Scherrer equation from the corresponding powder diffraction pattern (Fig. 2) was 4.3 ± 0.5 nm (Table 2). In addition, the diffraction pattern of this sample proves the formation of the expected product. The decomposition of the same precursor for 15 min gave similar results despite the reaction time being three times longer. The particle diameter distribution from TEM (Figures S9 and S10 in Suppl. Mater.) was 4.4 ± 1.1 nm again in good agreement with

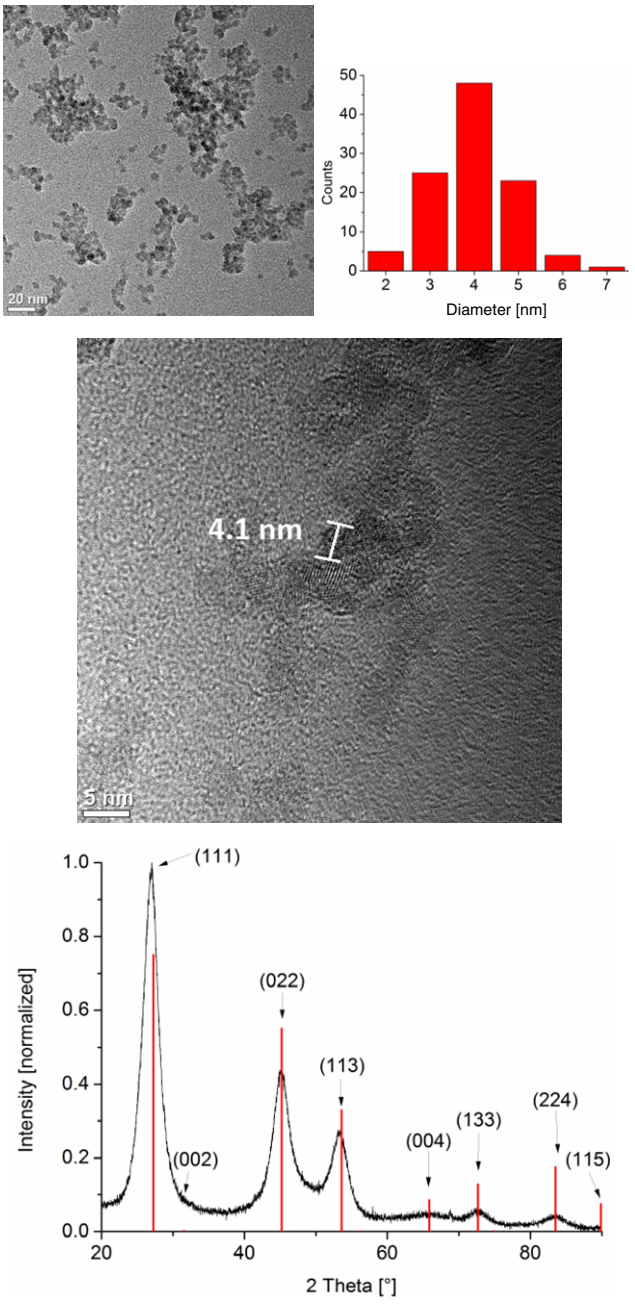

Fig. 2. HR-TEM images (top left and middle) of cubic ZnSe-NPs from decomposition of **3** (5 min, 250 °C) in [BMIm][BF_4], particle diameter distribution (top right) and PXRD-pattern (bottom) with cubic ZnSe reference (red COD-database: 9008879). (For interpretation of the references to color in this figure legend, the reader is referred to the web version of this article.)

the diameter determined from the powder diffraction pattern as 4.8 ± 1.0 nm.

Decomposition of the bis((alkylamino)alkylselenolato)zinc(II) complexes (**1**–**3**) led mostly to cubic ZnSe. Thereby impurities of

Table 2
Results of the microwave assisted synthesis of ZnSe NPs from **1–3** in [BMIm][BF_4].

Precursor	Ø-NPs TEM[a] (nm)	Ø-NPs PXRD[b] (nm)	ZnSe crystal system[c]	E_{gap} (eV)[d]
1 (5 min)	7.0 ± 1.9[e f]	4.0 ± 0.8[e]	hexagonal $P6_3mc$	3.02
1 (15 min)	5.0 ± 2.3[f]	4.2 ± 0.4	cubic F-43m	3.21
2 (5 min)	4.7 ± 1.3	4.3 ± 0.5	cubic F-43m	3.26
2 (15 min)	4.4 ± 1.1	4.8 ± 1.0	cubic F-43m	3.32
3 (5 min)	4.0 ± 0.9	4.2 ± 0.7	cubic F-43m	3.40
3 (15 min)	4.7 ± 2.1	4.5 ± 0.7	cubic F-43m	3.26

[a] Value with standard deviation σ.
[b] From the PXRD analysis of ZnSe-NPs with a Scherrer factor of 1.
[c] From the PXRD analysis of ZnSe-NPs (cubic ZnSe, reference: COD-database: 9008857; hexagonal ZnSe, reference: COD-database: 9008879).
[d] From Ø-NPs TEM with $m_e^* = 0.21\ m_e$, $m_h^* = 0.60\ m_e$ and E_{bulk} (at 300 °C) = 2.821 eV [57,58]; we chose the TEM diameter over the PXRD diameter as we view the TEM value as more accurate.
[e] The difference in the average particle diameter determined by TEM and by the Scherrer equation in case of precursor **1** (5min) is explained by peak broadening in the powder diffraction pattern due to the strain induced by crystal imperfection and distortions in the hexagonal (instead of cubic) crystal system.
[f] Concerning the decrease of size from TEM for NPs from **1** with increasing time we note the high variance (1σ). In view of this variance we cannot assign much significance to the diameter difference.

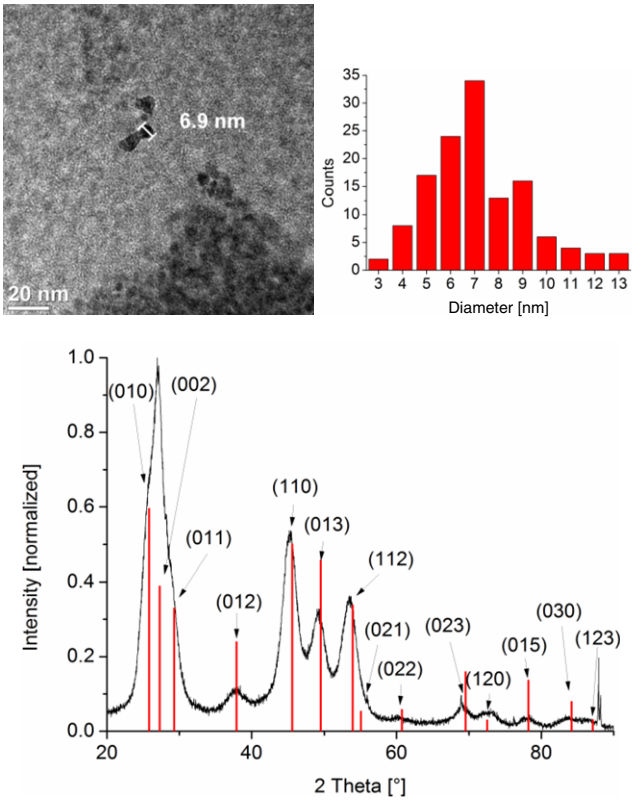

Fig. 3. HR-TEM image (top left) of hexagonal ZnSe-NPs from decomposition of **1** (5 min, 250 °C) in [BMIm][BF_4], particle diameter distribution (top right) and PXRD-pattern (bottom) with hexagonal ZnSe, reference (red COD-database: 9008879). (For interpretation of the references to color in this figure legend, the reader is referred to the web version of this article.)

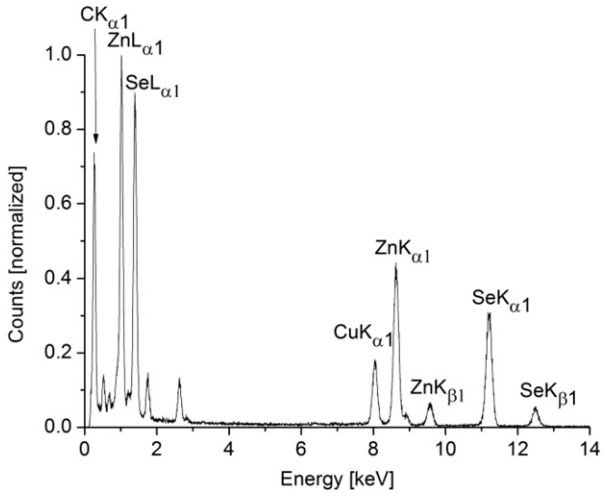

Fig. 4. EDX-spectrum of ZnSe-NPs from decomposition of **1** within 15 min.

hexagonal ZnSe cannot be ruled out due to the generally broad reflections and the appearance of a shoulder at about 50° 2-theta in the powder diffraction pattern.

The formation of hexagonal ZnSe particles could only be observed in case of the decomposition of **1** within 5 min. The phase change from cubic to hexagonal does not influence the particle size, as shown in Fig. 3. While the average diameter of the cubic ZnSe particles after 5 or 15 min decomposition time was typically between 4–5 nm (Table 2), the diameter of the hexagonal ZnSe nanoparticles was 7.0 nm. No additional stabilizing agents were necessary to reproducibly achieve such a small particle size. The significant difference in the average particle diameter determined by TEM and by Scherrer equation (Table 2) can be explained by peak broadening in the powder diffraction pattern due to the strain induced by crystal imperfection and distortions in the hexagonal crystal system.

For further characterization of the nanoparticles energy-dispersive X-ray spectra of each sample were recorded, as exemplified in Fig. 4. The spectrum shows, in addition to the signals of the carbon and copper containing sample holder no unexpected impurities. The quantification of the signals yields a molar ratio of nearly 1:1 for zinc and selenium, which also supports the formation of ZnSe nanoparticles.

Based on the "effective mass approximation" (EMA), Brus gave the first theoretical calculation for semiconductor nanoparticles [55]. By using a simplified form of the Brus equation (Eq. (1)) [56] the band gap energies of the synthesized ZnSe nanoparticles can be determined.

$$E_{gab} = E_{bulk} + \frac{h^2}{8r^2}\left[\frac{1}{m_e^*} + \frac{1}{m_h^*}\right]. \quad (1)$$

Here E_{bulk} is the band gap energy of the bulk material, h is Planck constant, r is the radius of the particle and m_e and m_h are the effective masses of the electron and the resulting hole. The calculated values of the band gap energies of the prepared ZnSe nanoparticles are listed in Table 2. Considering the small size of the synthesized particles a UV–Vis reflectance spectrum of the cubic ZnSe particles obtained by decomposition of **1** within 15 min was recorded as an example (Fig. 5). The particles were precipitated

Table 3
Thermal analysis of the cadmium precursors (**4–6**) and analysis of the resulting residues by PXRD.

Precursor	Δm (%)	$\Delta m_{theor.}$ (%)	Decomp. temp. (° C)	CdSe crystal system[a]
4	38	35	150	hexagonal $P6_3mc$
5	39	39	165	hexagonal $P6_3mc$
6	39	39	155	hexagonal $P6_3mc$

[a] From PXRD analysis of the residue of the thermal analysis (hexagonal CdSe, reference: COD-database: 9008863).

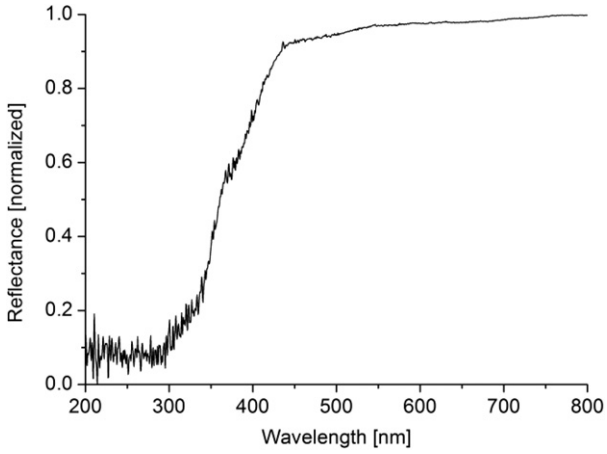

Fig. 5. UV–Vis reflectance spectrum of freshly prepared ZnSe-NPs from decomposition of **1** within 15 min.

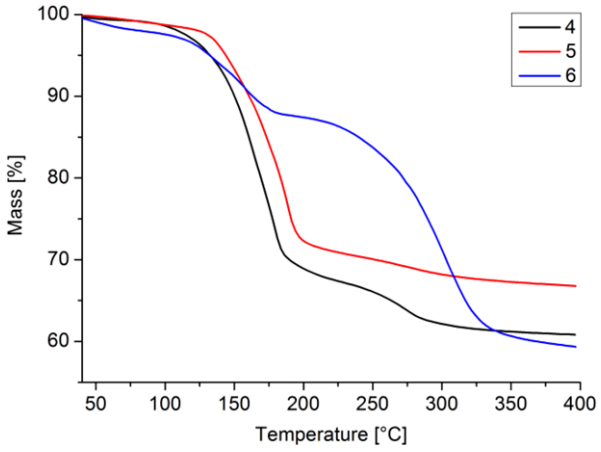

Fig. 6. Thermogravimetric analyses of bis((dialkylamino)alkylselenolato)cadmium(II) complexes (**4–6**).

upon addition of acetonitrile. The UV–Vis reflectance spectrum shows an absorption edge at 371 nm (at the inflection point). From $E = h \cdot c/\lambda$ this translates into a band gap energy of the particles of 3.34 eV, which corresponds relatively well to the calculated value of 3.21 eV (Table 2).

In all prepared ZnSe samples no significant fluorescence could be observed upon irradiation with a UV lamp of the precipitated nanoparticles.

2.4. Thermogravimetric analysis of Cd complexes **4–6**

For the bis((dialkylamino)alkylselenolato)cadmium(II) complexes (**4–6**) the thermogravimetric analysis (Fig. 6) indicates a lower decomposition temperature as the respective zinc complexes. The Cd complexes already start to decompose at temperatures of about 160 °C, which corresponds to known selenolate complexes of cadmium [12]. The residual mass (Δm) matches the expected values for CdSe ($\Delta m_{\text{theor.}}$) (Table 3). The formation of hexagonal CdSe as decomposition product was positively identified by X-ray powder diffraction (Figure S2 in Suppl. Mater.).

2.5. CdSe-NPs in [BMIm][BF_4]

CdSe/IL nanoparticle dispersions were obtained in the same manner as described above for the ZnSe nanoparticles. A defined amount of the precursor was suspended in ionic liquid and then decomposed by microwave assisted heating for 5 or 15 min at 250 °C as shown in Scheme 3.

Fig. 7 shows the CdSe particles obtained by decomposition of **6** within 5 min. The microwave assisted synthesis led to agglomerated, spherical and crystalline particles of hexagonal CdSe. The particle diameter distribution of the sample by TEM was 9.3 ± 1.3 nm, matching the particle diameter determined by the Scherrer equation as 7.9 ± 0.7 nm (Table 3).

The decomposition of the same precursor (**6**) for 15 min showed similar results with a particle diameter distribution (Figures S28

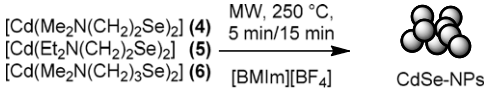

Scheme 3. Decomposition of the bis((dialkylamino)alkylselenolato)cadmium(II) complexes (**4–6**).

and S29 in Suppl. Mater.) of 10.9 ± 1.7 nm and a diameter determined from the powder diffraction pattern by the Scherrer equation of 7.8 ± 0.5 nm. The decomposition of bis((dialkylamino)alkylselenolato)cadmium(II) complexes led to the formation of hexagonal CdSe with an average particle diameter between 10–19 nm. In comparison to the ZnSe particles, the obtained CdSe nanoparticles were not only larger, also the overall particle diameter distribution was wider, as can been seen in Table 4. A significant amount of strain on the lattice structure of the CdSe particles was determined to be responsible for peak broadening in the powder diffraction patterns, which can also be confirmed by the formation of an additional reflection at ~61° 2-theta. The extent of the strain was approximately calculated by a Williamson–Hall analysis considering a Pseudo-Voigt function and a Scherrer factor of 1 [59,60] as listed in Table 4. Even when the strain correction is taken into account, the corrected PXRD particle diameters differ from the TEM ones, which indicates an anisotropic amount of defects in the particles. The occurrence of defects in the crystal system, as well as their larger diameter may be induced by the reaction temperature and the reaction time.

For further characterization energy-dispersive X-ray spectra were recorded for each sample as exemplified in Fig. 8. Except for the signals of carbon and copper, which originate from the sample holder, only signals for cadmium and selenium can be seen. The quantification of the signals shows a molar ratio of nearly 1:1 for cadmium and selenium in each case. This is also evidence for the formation of CdSe nanoparticles.

From the example of an UV–Vis reflectance spectrum of the CdSe particles obtained from of **4** within 5 min. (Fig. 9) with an absorption edge at 691 nm a band gab energy of 1.79 eV was

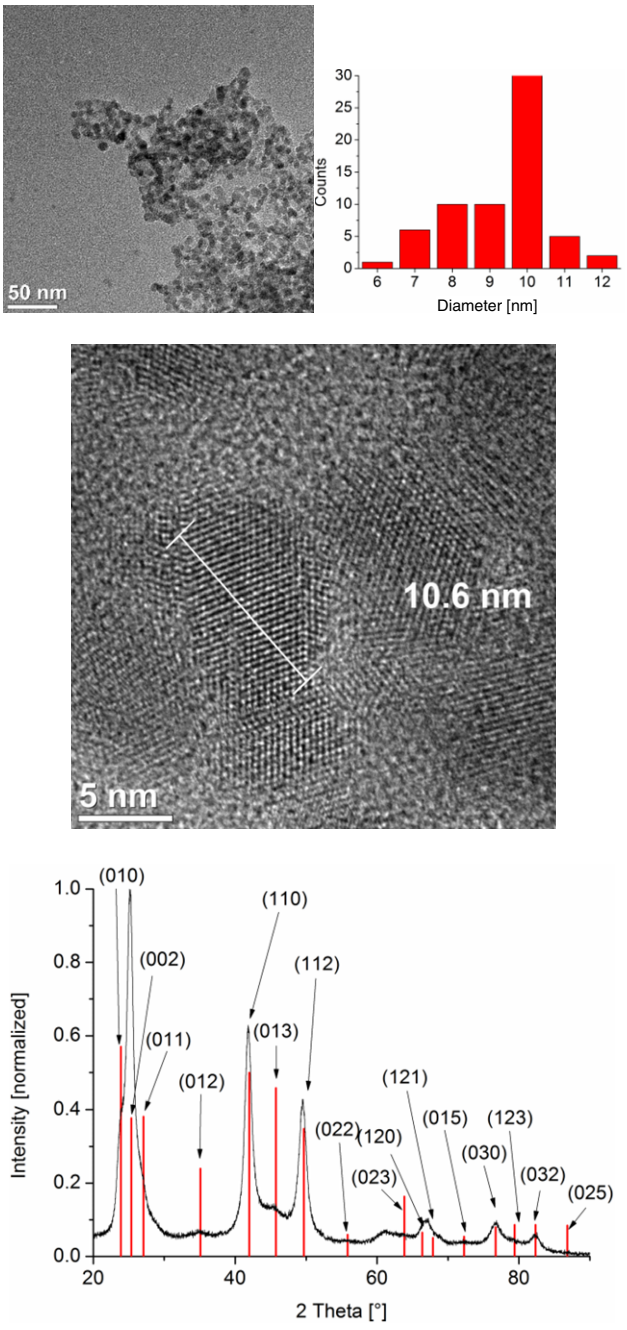

Fig. 7. CdSe-NPs from decomposition of **6** (5 min, 250 °C). HR-TEM images (top left and bottom), particle diameter distribution (top right) and PXRD-pattern (hexagonal CdSe, reference (red): COD-database: 9008863). Additional TEM images are given in Figure S26. (For interpretation of the references to color in this figure legend, the reader is referred to the web version of this article.)

calculated. This matches the value of 1.79 eV calculated from the particle diameter using the simplified Brus equation (Table 4).

Also in case of the CdSe nanoparticles no significant fluorescence could be observed upon UV-irradiation of the precipitated particles.

3. Conclusions

Aminoalkylselenolate metal precursors are well suited for the microwave-assisted synthesis of ZnSe and CdSe nanoparticles in ionic liquids. In all cases nanoparticles could be obtained without the use of other stabilizing agents besides the IL. Hexagonal and

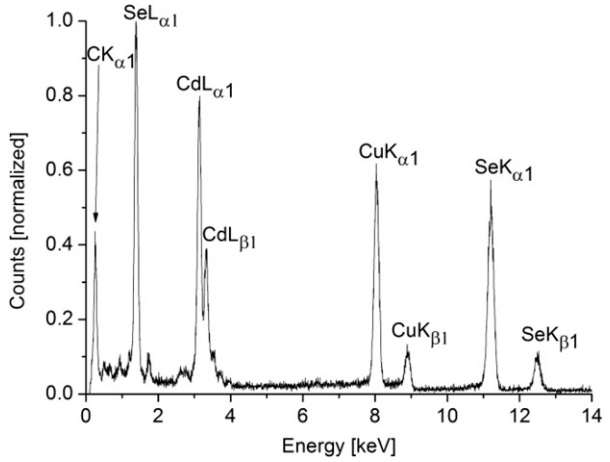

Fig. 8. EDX-spectrum of CdSe-NPs from decomposition of **4** within 15 min.

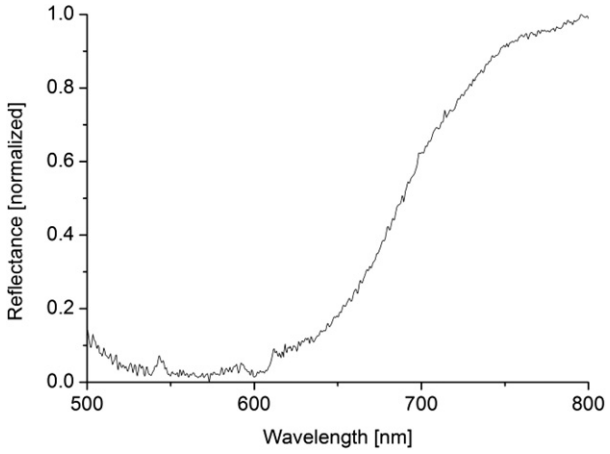

Fig. 9. UV–Vis reflectance spectrum of freshly prepared CdSe-NPs from decomposition of **4** within 5 min.

cubic ZnSe with a particle diameter between 4–7 nm were prepared. From the cadmium precursors hexagonal CdSe nanoparticles with an average particle diameter of 10–19 nm were obtained. No metal fluorides are observed despite the use of a fluorous IL (different from seen before in the dual source approach). Slight variations in ligand system or different decomposition times do only affect the particle diameter of the CdSe nanoparticles. For the cubic ZnSe particles there seems to be no influence, which is different from other known syntheses [1,15]. Furthermore there seems to be some strain to the hexagonal crystal system of ZnSe and CdSe, which in case of the CdSe particles may be caused by the high reaction temperature. For the chosen conditions it can be assumed that the ionic liquid has the decisive influence on the size, shape and crystallinity of the particles.

4. Experimental section

4.1. General remarks

Standard Schlenk techniques under inert gas atmosphere (N_2) were used for the syntheses of the Complexes. Methanol and n-hexane were dried over molecular sieves 3 Å; other common solvents were of solvent grade quality. 3-Dimethylamino-1-propyl chloride hydrochloride 99%, 2-Dimethylamino-1-ethyl chloride hydrochloride 99% and 2-Diethylamino-1-ethyl chloride hydrochloride 99% were received by Acros Organics, potassium borohydride 99.99% by Merck, selenium powder 99.99% by Strem,

Table 4
Results of the microwave assisted synthesis of CdSe-NPs.

Precursor	Ø-NPs TEM[a] (nm)	Ø-NPs PXRD[b] (nm)	Non-linear strain[c] (%)	Ø-NPs PXRD W-H[bc] (nm)	CdSe crystal system[d]	E_{gap} (eV)[e]
4 (5 min)	15.4 ± 1.5	10.5 ± 1.3	0.38 ± 0.09	14.7 ± 2.1	hexagonal $P6_3mc$	1.79
4 (15 min)	18.9 ± 3.3	8.0 ± 1.8	0.67 ± 0.31	11.4 ± 3.3	hexagonal $P6_3mc$	1.76
5 (5 min)	11.9 ± 2.5	11.6 ± 0.8	0.91 ± 0.27	15.6 ± 4.9	hexagonal $P6_3mc$	1.82
5 (15) min	18.6 ± 2.9	9.6 ± 1.3	0.57 ± 0.15	15.1 ± 3.1	hexagonal $P6_3mc$	1.76
6 (5 min)	9.3 ± 1.3	7.9 ± 0.7	0.53 ± 0.25	11.8 ± 2.0	hexagonal $P6_3mc$	1.89
6 (15 min)	10.9 ± 1.7	7.8 ± 0.5	0.63 ± 0.15	11.1 ± 1.8	hexagonal $P6_3mc$	1.84

[a] Value with standard deviation σ.
[b] From the PXRD analysis of CdSe-NPs with a Scherrer factor of 1.
[c] From Williamson–Hall plot (Pseudo-Voigt).
[d] From the PXRD analysis of CdSe-NPs (hexagonal CdSe, reference: COD-database: 9008863).
[e] From Ø-NPs TEM with $m_e* = 0.14\ m_e$, $m_h^* = 0.45\ m_e$ and E_{bulk} (at 300° C) = 1.714 eV [61]; we chose the TEM diameter over the PXRD diameter as we view the TEM value as more accurate.

zinc(II) acetate dihydrate, cadmium(II) acetate dihydrate by Merck. The IL 1-butyl-3-methyl-imidazolium tetrafluoridoborate was synthesized from 1-methylimidazol following the literature [62].

4.2. Instrumentation

The synthesis of metal selenide nanoparticles was carried out by decomposition of the precursors in the CEM Discover microwave reactor system.

The ^{1}H-, ^{13}C- and ^{77}Se-NMR-spectra were measured on an Avance III-600 or a Bruker Avance III-300 NMR-spectrometer at 298 K. For the ^{77}Se-NMR-measurements a standard solution of KSeCN in D_2O was used.

The thermal analyses were performed on a NETSCH TG Tarsus 300 with a heating rate of 5 K/min.

The measurements of the PXRD-patterns were done at room temperature on a Bruker D2 phaser in 2-theta angles with a Cu-Kα-radiation (λ = 1.54182 Å) at a voltage of 35 kV.

HR-TEM-images and EDX-spectra were collected at the Ernst-Ruska Centre Jülich for Microscopy and Spectroscopy with Electrons (Jülich Research Centre and RWTH Aachen University) on a FEI Tecnai G2 F20 with an acceleration voltage of 200 kV. The particle diameter distributions were determined by Gatan digital micrograph software.

The UV–Vis reflectance spectra were recorded on a SPECORD S600 from Analytik Jena using an integration sphere at ambient temperature.

4.3. General synthesis of the diselenides

In a 250 ml Schlenk-flask 8.00 g selenium (100 mmol) were suspended in 50.0 ml of water. To this suspension 4.00 g NaOH (100 mmol) and 0.50 and 0.50 g (14 mmol) of $NaBH_4$ dissolved in 10 ml of water were added, resulting in a dark red solution. The mixture was stirred for 1 h at room temperature and then 30 min at 90 °C until the selenium was dissolved completely. After cooling to room temperature the solution was treated with an aqueous solution of one equivalent (100 mmol) of the respective aminoalkyl chloride hydrochloride and 4.00 g (100 mmol) NaOH. The reaction mixture was again stirred 1 h at 70 °C. The reaction mixture was extracted with 20 ml of n-hexane three times, the combined organic phases were treated with magnesium sulfate and the solvent was removed. Finally the oily orange–red product was dried in vacuum.

(Dimethylamino)ethyldiselenide ($[\mathbf{Me_2N(CH_2)_2Se}]_2$)

Yield: 84%–95%, Lit. [54]: 72%; ^{1}H-NMR (300 MHz, $CDCl_3$): δ [ppm] = 2.17 (s, 12 H, CH_3); 2.55 (t, ^3J = 7.0 Hz, 4 H, $SeCH_2$); 2.96 (t, ^3J = 7.0 Hz, 4 H, NCH_2); ^{13}C-NMR (75 MHz, $CDCl_3$): δ [ppm] = 28.3 ($SeCH_2$); 45.2 (CH_3); 60.3 (NCH_2); ^{77}Se-NMR (57 MHz, $CDCl_3$): δ [ppm] = 295.0; MS (EI, 70 eV): m/z = 305 $[C_8H_{20}N_2Se_2 + H]^+$; 233 $[C_4H^{11}NSe_2]^{+\bullet}$; 153 $[C_4H_{11}NSe]^{+\bullet}$; 73 $[C^4H_{11}N]^{+\bullet}$; 58 $[C_4H_{10}]^{+\bullet}$; 45 $[C_2H_6N]^{+\bullet}$.

(Diethylamino)ethyldiselenide ($[\mathbf{Et_2N(CH_2)_2Se}]_2$)

Yield: 71%–75%; ^{1}H-NMR (600 MHz, $CDCl_3$): δ [ppm] = 2.18 (t, ^3J = 7.6 Hz, 12 H, CH_3); 2.48 (t, ^3J = 7.6 Hz, 4 H, $SeCH_2$); 2.56 (q, ^3J = 7.3 Hz, 8 H, CH_2); 2.64 (t, ^3J = 7.4 Hz, 4 H, NCH_2); ^{13}C-NMR (150 MHz, $CDCl_3$): δ [ppm] = 11.1 (CH_3) 20.3 ($SeCH_2$); 46.0 (CH_2); 52.9 (NCH_2); ^{77}Se-NMR (75 MHz, $CDCl_3$): δ [ppm] = 294.85; MS (EI, 70 eV): m/z = 261 $[C_6H_{15}NSe_2]^{+\bullet}$; 181 $[C_6H_{15}NSe]^{+\bullet}$; 100 $[C_6H_{14}N]^+$; 86 $[C_5H_{12}N]^+$; 58 $[C_4H_{10}]^{+\bullet}$.

(Dimethylaminopropyl)diselenide ($[\mathbf{Me_2N(CH_2)_3Se}]_2$)

Yield: 82%–96%, Lit. [54]: 68%; ^{1}H-NMR (300 MHz, $CDCl_3$): δ [ppm] = 1.82 (quin, ^3J = 7.2 Hz, 4 H, CH_2); 2.13 (s, 12 H, CH_3); 2.26 (t, ^3J = 7.1 Hz, 4 H, $SeCH_2$); 2.87 (t, ^3J = 7.2 Hz, 2 H, NCH_2); ^{13}C-NMR (75 MHz, $CDCl_3$): δ [ppm] = 27.7 ($SeCH_2$); 28.8 (CH_2); 45.9 (CH_3); 59.0 (NCH_2); ^{77}Se-NMR (57 MHz, $CDCl_3$): δ [ppm] = 314, 3; MS (EI, 70 eV): m/z = 167 $[C_5H_{13}NSe]^{+\bullet}$; 166 $[C_5H_{12}NSe]^{+\bullet}$; 137 $[C_4H_{10}Se]^{+\bullet}$; 87 $[C_5H_{13}N]^{+\bullet}$; 58 $[C_4H_{10}]^{+\bullet}$.

4.4. General synthesis of the zinc and cadmium complexes

In a 100 ml Schlenk-flask 5.00 mmol of the respective diselenide was solved in 10 ml of dry methanol. Under nitrogen atmosphere 12.38 g (10.0 mmol) $NaBH_4$ was added, resulting in a discoloration of the solution under the formation of hydrogen gas. The selenolate solution was then added drop wise to either a suspension of 5.00 mmol $Zn(OAc)_2 \cdot 2H_2O$ or $Cd(OAc)_2 \cdot 2H_2O$ in 50 ml of dichloromethane or to a solution of the appropriate salt in methanol. The reaction mixture was stirred for 3 h at room temperature. The solvent was removed via rotary evaporation and the resulting residue was taken up with 80 ml of dichloromethane, filtered and washed again with 20 ml of dichloromethane. The resulting pale yellow solution was allowed to stand for crystallization, that a pale yellow microcrystalline solid was obtained.

$[\mathbf{Zn(Me_2N(CH_2)_2Se)_2}]$(1)

Yield: 59%–78%, Lit. [13]: 65%; ^{1}H-NMR (300 MHz, $CDCl_3$): δ [ppm] = 2.26 (s, 12 H, CH_3); 2.64 (t, ^3J = 7.5 Hz, 4 H, $SeCH_2$); 3.06 (t, ^3J = 7.5 Hz, 4 H, NCH_2); ^{13}C-NMR (75 MHz, $CDCl_3$): δ [ppm] = 12.7 ($SeCH_2$); 45.3 (CH_3); 63.2 (NCH_2); TGA (Heating rate: 5 °C/min): Decomp. [° C] = 210; Δm [%] = 43 (39 theor.).

$[\mathbf{Zn(Et_2N(CH_2)_2Se)_2}]$(2)

Yield: 25%–35%; ^{1}H-NMR (300 MHz, $CDCl_3$): δ [ppm] = 0.72 (t, ^3J = 7.1 Hz, 12 H, CH_3); 2.32 (q, ^3J = 7.1 Hz, 8 H, CH_2); 2.50 (t, ^3J = 7.2 Hz, 4 H, $SeCH_2$); 2.64 (t, ^3J = 7.0 Hz, 4 H, NCH_2); ^{13}C-NMR (75 MHz, $CDCl_3$): δ [ppm] = 11.1 (CH_3); 20.3 ($SeCH_2$); 46.0 (CH_2); 52.9 (NCH_2); TGA (Heating rate: 5 °C/min): Decomp. [°C] = 210; Δm [%] = 48 (45 theor.).

[$Zn(Me_2N(CH_2)_3Se)_2$](3)

Yield: 58%–67%; ^{1}H-NMR (300 MHz, $CDCl_3$): δ [ppm] = 1.61 (quin, ^3J = 7.0 Hz, 4 H, CH_2); 1.92 (s, 12 H, CH_3); 2.0 (t, ^3J = 6.8 Hz, 2 H, $SeCH_2$); 2.64 (t, ^3J = 7.2 Hz, 2 H, NCH_2); ^{13}C-NMR (75 MHz, $CDCl_3$): δ [ppm] = 27.1 ($SeCH_2$); 28.1 (CH_2); 44.8 (CH_2); 58.32 (NCH_2); TGA (Heating rate: 5 °C/min): Decomp [°C] = 210; Δm [%] = 43 (43 theor.).

[$Cd(Me_2N(CH_2)_2Se)_2$](4)

Yield: 51%, Lit. [12]: 68%; ^{1}H-NMR (300 MHz, $CDCl_3$): δ [ppm] = 2.27 (s, 12 H, CH_3); 2.65 (t, ^3J = 7.2 Hz, 4 H, $SeCH_2$); 3.05 (t, ^3J = 7.2 Hz, 4 H, NCH_2); ^{13}C-NMR (75 MHz, $CDCl_3$): δ [ppm] = 28.1 ($SeCH_2$); 45.1 (CH_3); 60.3 (NCH_2); TGA (Heating rate: 5 °C/min): Decomp. [°C] = 155; Δm [%] = 38 (35 theor.).

[$Cd(Et_2N(CH_2)_2Se)_2$](5)

Yield: 17%–32%; ^{1}H-NMR (300 MHz, $CDCl_3$): δ [ppm] = 0.81 (t, ^3J = 6.9 Hz, 12 H, CH_3); 2.32 (q, ^3J = 7.0 Hz, 8 H, CH_2); 2.37–2.67 (m, 8 H, $SeCH_2$ & NCH_2); ^{13}C-NMR (75 MHz, $CDCl_3$): δ [ppm] = 11.4 (CH_3) 20.8 ($SeCH_2$); 46.3 (CH_2); 53.3 (NCH_2); TGA (Heating rate: 5 °C/min): Decomp. [°C] = 185; Δm [%] = 34 (42 theor.).

[$Cd(Me_2N(CH_2)_3Se)_2$](6)

Yield: 18%; ^{1}H-NMR (300 MHz, $CDCl_3$): δ = 1.90 (quin, ^3J = 7.2 Hz, 4 H, CH_2); 2.21 (s, 12 H, CH_3); 2.35 (t, ^3J = 7.1 Hz, 2 H, $SeCH_2$); 2.94 (t, ^3J = 7.4 Hz, 2 H, NCH_2); ^{13}C-NMR (75 MHz, $CDCl_3$): δ [ppm] = 27.1 ($SeCH_2$); 28.1 (CH_2); 44.8 (CH_3); 58.3 (NCH_2); TGA (Heating rate: 5 °C/min): Decomp. [°C] = 225; Δm [%] = 39 (39 theor.).

4.5. General synthesis of ZnSe- and CdSe-NPs in [BMIm][BF_4]

Dispersions with 1-mass% of the respective metal selenide in ionic liquid were received by suspending the required amount of the corresponding selenolate complex in [BMIm][BF_4]. The decomposition was carried out under microwave irradiation (40 W, 250 °C) for either 5 or 15 min. The gaseous byproducts were removed under reduced pressure. For the analysis of the particles, they were first precipitated with acetonitrile, and then washed several times.

Acknowledgment

Authors are thankful to the Deutsche Forschungsgemeinschaft (DFG) for grant Ja466/31-1 within the priority project SPP 1708.

Appendix A. Supplementary data

Supplementary material related to this article can be found online at http://dx.doi.org/10.1016/j.nanoso.2015.06.001.

References

[1] M.L. Landry, T.E. Morrell, T.K. Karagounis, C.-H. Hsia, C.Y. Wang, J. Chem. Educ. 91 (2014) 274–280.
[2] W. Huynch, X.G. Peng, A.P. Alivisatos, Adv. Mater. 11 (1999) 923–928.
[3] C.E. Fritts, Dingler's Polytechnisches J. 258 (1886) 44–45.
[4] (a) W.C.W. Chan, S. Nie, Science 281 (1998) 2016–2020;
(b) D.R. Larson, W.R. Zipfel, R.W. Williams, S.W. Clark, M.P. Bruchez, F.W. Wise, W.W. Webb, Science 300 (2003) 1434–1438;
(c) M. Green, Angew. Chem. Int. Ed. 43 (2004) 4129–4132;
(d) S.P. Mucur, T.A. Tumay, S. Birdogan, S.E. San, E. Tekin, Nano-Struct. Nano-Objects 1 (2015) 7–14.
[5] M. Brust, J. Fink, B. Bethel, D.J. Schriffren, M. Kiely, J. Chem. Soc. Chem. Commun. (1995) 1655–1657.
[6] J. Tanori, M.P. Pileni, Adv. Mater. 7 (1995) 862–865.
[7] R.A. Andrievskii, Russ. Chem. Rev. 63 (1994) 411–427.
[8] J.A. Smyder, T.D. Krauss, Mater. Today 14 (2011) 382–388.
[9] G. Xiao, Y. Wang, J. Ning, Y. Wei, B. Liu, W.W. Yu, G. Zou, B. Zou, RSC Adv. 3 (2013) 8104–8131.
[10] A. Rubin-Brusilovski, G. Maikov, D. Kolan, R. Vaxenburg, J. Tilchin, Y. Kauffmann, A. Sashchiuk, E. Lifshitz, J. Phys. Chem. C 116 (2012) 18983–18990.
[11] J. Tang, L. Brzozowski, D.A.R. Barkhouse, X. Wang, R. Debnath, R. Wolowiec, E. Palmiano, L. Levina, A.G. Pattantyus-Abraham, D. Jamakosmanovic, E.H. Sargent, ACS Nano 4 (2010) 869–879.
[12] G. Kedarnath, S. Dey, V.K. Jain, G.K. Dey, B. Varghese, Polyhedron 25 (2006) 2383–2392.
[13] S. Dey, V.K. Jain, S. Chaudhury, A. Knoedler, W. Kaim, Polyhedron 22 (2003) 489–492.
[14] G. Kedarnath, L.B. Kumbhare, S. Dey, A.P. Wadawale, V.K. Jain, G.K. Dey, Polyhedron 28 (2009) 2749–2754.
[15] A. Guleria, A.K. Singh, M.C. Rath, S.K. Sarkar, S. Adhikari, Dalton Trans. 43 (2014) 11843–11844.
[16] Z. Li, Z. Jia, Y. Luan, T. Mu, Curr. Opin. Solid State Mater. Sci. 12 (2008) 1–8.
[17] M. Antonietti, D. Kuang, B. Smarsly, Y. Zhou, Angew. Chem. Int. Ed. 43 (2004) 4988–4993.
[18] K. Schütte, A. Doddi, C. Kroll, H. Meyer, C. Gemel, G. van Tendeloo, R.A. Fischer, C. Janiak, Nanoscale 6 (2014) 5532–5544.
[19] K. Schütte, H. Meyer, C. Gemel, J. Barthel, R.A. Fischer, C. Janiak, Nanoscale 6 (2014) 3116–3126.
[20] D. Marquardt, F. Beckert, F. Pennetreau, F. Tölle, R. Mülhaupt, O. Riant, S. Hermans, J. Barthel, C. Janiak, Carbon 66 (2014) 285–294.
[21] D. Marquardt, J. Barthel, M. Braun, C. Ganter, C. Janiak, CrystEngComm 14 (2012) 7607–7615.
[22] M.F. Groh, U. Müller, E. Ahmed, A. Rothenberger, M. Ruck, Z. Naturforsch. B 68 (2013) 1108–1122.
[23] E. Ahmed, J. Breternitz, M.F. Groh, M. Ruck, CrystEngComm 14 (2012) 4874–4885.
[24] H. Zou, Y. Luan, J. Ge, Y. Wang, G. Zhuang, R. Li, Z. Li, CrystEngComm 13 (2011) 2656–2660.
[25] A. Taubert, F. Stange, Z. Li, M. Junginger, C. Günter, M. Neumann, A. Friedrich, ACS Appl. Mater. Interfaces 4 (2012) 791–795.
[26] T. Alamma, A. Birkner, A.-V. Mudring, Eur. J. Inorg. Chem. (2009) 2765–2768.
[27] B. Rodríguez-Cabo, E. Rodil, H. Rodríguez, A. Soto, A. Arce, Angew. Chem. Int. Ed. 51 (2012) 1424–1427.
[28] Y. Lin, S. Dehnen, Inorg. Chem. 50 (2011) 7913–7915.
[29] Y. Lin, W. Massa, S. Dehnen, J. Am. Chem. Soc. 134 (2012) 4497–4500.
[30] E. Ahmed, M. Ruck, Dalton. Trans. 40 (2011) 9347–9357.
[31] W.-W. Xiong, J.-R. Li, B. Hu, B. Tan, R.-F. Li, X.-Y. Huang, Chem. Sci. 3 (2012) 1200–1204.
[32] C. Janiak, Metal nanoparticle synthesis in ionic liquids, in: J. Dupont, L. Kollar (Eds.), Ionic Liquids (ILs) in Organometallic Catalysis, Springer, Heidelberg, 2014, ISSN 1436–6002.
[33] C. Janiak, Metal nanoparticle synthesis in ionic liquids, in: C. Hardacre, V. Parvulescu (Eds.), Catalysis in Ionic Liquids: From Catalyst Synthesis to Application, RSC Publishing, Cambridge, 2014, pp. 537–577. Chapter 11, ISBN: 978-1-84973-603-9.
[34] C. Janiak, Z. Naturforsch. B 68 (2013) 1056–1059.
[35] H.G. Zhu, J.F. Huang, Z.W. Pan, S. Dai, Chem. Mater. 18 (2006) 4473–4477.
[36] Y. Wang, H. Yang, J. Am. Chem. Soc. 127 (2005) 5316–5318.
[37] Y. Wang, H. Yang, Chem. Commun. (2006) 2545–2548.
[38] X. Zhou, Z.-X. Xie, Z.-Y. Jiang, Q. Kuang, S.-H. Zhang, T. Xu, R.B. Huang, L.-S. Zheng, Chem. Commun. (2005) 5572–5575.
[39] (a) J. Jiang, S. Yu, W. Yao, H. Ge, G. Zhang, Chem. Mater. 17 (2005) 6094–6100;
(b) G.S. Fonseca, G. Machado, S.R. Teixeira, G.H. Fecher, J. Morais, M.C.M. Alves, J. Dupont, J. Colloid Interface Sci. 301 (2006) 193–205.
[40] S. Dai, Y.H. Ju, H.J. Gao, J.S. Lin, S.J. Pennycook, C.E. Barnes, Chem. Commun. (2000) 243–245.
[41] T. Nakashima, N. Kimizuka, J. Am. Chem. Soc. 125 (2003) 6386–6388.
[42] J.F. Huang, I.-W. Sun, Adv. Funct. Mater. 15 (2005) 989–994.
[43] S. Zein El Abedin, N. Borissenko, F. Endres, Electrochem. Commun. 6 (2004) 510–515.
[44] T. Tsuda, T. Sakamoto, Y. Nishimura, S. Seino, A. Imanishi, S. Kuwabata, Chem. Commun. 48 (2012) 1925–1927.
[45] T. Tsuda, T. Sakamoto, Y. Nishimura, S. Seino, A. Imanishi, K. Matsumoto, R. Hagiwara, T. Uematsu, S. Kuwabata, RSC Adv. 2 (2012) 11801–11808.
[46] S. Chen, Y. Liu, G. Wu, Nanotechnology 16 (2005) 2360–2366.
[47] Z. Li, Z. Liu, J. Zhang, B. Han, J. Du, Y. Gao, T. Jiang, J. Phys. Chem. B 109 (2005) 14445–14449.
[48] Y. Jiang, Y.-J. Zhu, G.-F. Cheng, Cryst. Growth Des. 6 (2006) 2174–2177.
[49] L.-X. Yang, Y.-J. Zhu, W.-W. Wang, H. Tong, M.-L. Ruan, J. Phys. Chem. B 110 (2006) 6609–6614.
[50] Y. Jiang, Y.-J. Zhu, J. Phys. Chem. B 109 (2005) 4361–4364.
[51] O. Hoefft, F. Endres, Phys. Chem. Chem. Phys. 13 (2011) 13472–13478.
[52] Y.M. Song, D.M. Jang, K.Y. Park, J. Park, E.H. Cha, J. Korean Electrochem. Soc. 14 (2011) 1–8.
[53] S.I. Abu-Eishah, Ionic Liquids Recycling for Reuse, Ionic Liquids—Classes and Properties S. Handy (Ed.), 2011, p. 249–272 ISBN: 978-953-307-634-8.
[54] (a) S. Dey, V.K. Jain, S. Chaudhury, A. Knoedler, F. Lissner, W. Kaim, Dalton Trans. (2001) 723–728;
(b) S. Dey, V.K. Jain, A. Knoedler, W. Kaim, Inorg Chim Acta 349 (2003) 104–110.
[55] L.E. Brus, J. Chem. Phys. 80 (1984) 4403–4411.
[56] E.O. Chukwuocha, M.C. Onyeaju, T.S.T. Harry, World J. Condensed Matter Phys. 2 (2012) 96–100.
[57] J. Singh, Physics of Semiconductors and Their Heterostructures, McGraw-Hill, New York, 1993.
[58] O. Madelung, Data in Science and Technology: Semiconductors, Springer, Heidelberg, 1991.
[59] V.D. Mote, Y. Purushotham, B.N. Dole, J. Theor. Appl. Phys. 6 (2012) 1–8.
[60] C. Suryanarayana, M. Grant, Norton: X-ray Diffraction: A Practical Approach, Springer, New York, 1998.
[61] L. Brus, J. Phys. Chem. 90 (12) (1986) 2555–2560.
[62] X. Creary, E.D. Willis, Org. Synth. (2005) 166–169.